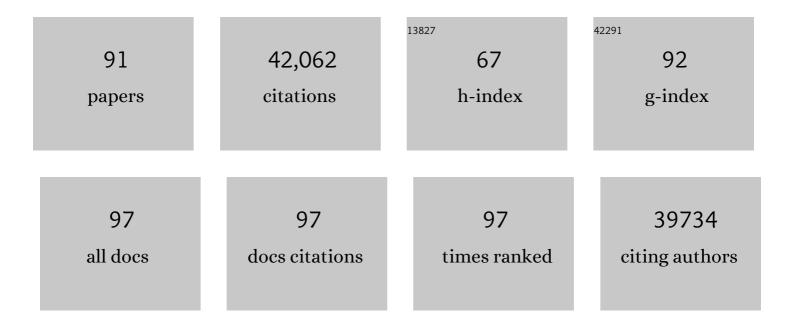
List of Publications by Year in descending order

Source: https://exaly.com/author-pdf/4744377/publications.pdf Version: 2024-02-01



#	Article	IF	CITATIONS
1	Highly Reversible Zn Metal Anode Stabilized by Dense and Anionâ€Derived Passivation Layer Obtained from Concentrated Hybrid Aqueous Electrolyte. Advanced Functional Materials, 2022, 32, 2103959.	7.8	48
2	High-precision tumor resection down to few-cell level guided by NIR-IIb molecular fluorescence imaging. Proceedings of the National Academy of Sciences of the United States of America, 2022, 119, e2123111119.	3.3	26
3	Probing dissolved CO ₂ (aq) in aqueous solutions for CO ₂ electroreduction and storage. Science Advances, 2022, 8, eabo0399.	4.7	17
4	In vivo non-invasive confocal fluorescence imaging beyond 1,700 nm using superconducting nanowire single-photon detectors. Nature Nanotechnology, 2022, 17, 653-660.	15.6	88
5	In vivo NIR-II structured-illumination light-sheet microscopy. Proceedings of the National Academy of Sciences of the United States of America, 2021, 118, .	3.3	39
6	Selective and High Current CO ₂ Electro-Reduction to Multicarbon Products in Near-Neutral KCl Electrolytes. Journal of the American Chemical Society, 2021, 143, 3245-3255.	6.6	108
7	Rational Design of High Brightness NIR-II Organic Dyes with S-D-A-D-S Structure. Accounts of Materials Research, 2021, 2, 170-183.	5.9	84
8	Rechargeable Na/Cl2 and Li/Cl2 batteries. Nature, 2021, 596, 525-530.	13.7	103
9	Sub-10-nm graphene nanoribbons with atomically smooth edges from squashed carbon nanotubes. Nature Electronics, 2021, 4, 653-663.	13.1	61
10	Tuning Dynamically Formed Active Phases and Catalytic Mechanisms of <i>In Situ</i> Electrochemically Activated Layered Double Hydroxide for Oxygen Evolution Reaction. ACS Nano, 2021, 15, 14996-15006.	7.3	56
11	Exploring the performance of carbonate and ether-based electrolytes for anode-free lithium metal batteries operating under various conditions. Journal of Power Sources, 2021, 512, 230388.	4.0	6
12	Deep learning for in vivo near-infrared imaging. Proceedings of the National Academy of Sciences of the United States of America, 2021, 118, .	3.3	53
13	Ionic Liquid Analogs of AlCl ₃ with Urea Derivatives as Electrolytes for Aluminum Batteries. Advanced Functional Materials, 2020, 30, 1901928.	7.8	74
14	Crossâ€Linkâ€Functionalized Nanoparticles for Rapid Excretion in Nanotheranostic Applications. Angewandte Chemie, 2020, 132, 20733-20741.	1.6	6
15	Crossâ€Linkâ€Functionalized Nanoparticles for Rapid Excretion in Nanotheranostic Applications. Angewandte Chemie - International Edition, 2020, 59, 20552-20560.	7.2	35
16	Molecular engineering of dispersed nickel phthalocyanines on carbon nanotubes for selective CO2 reduction. Nature Energy, 2020, 5, 684-692.	19.8	365
17	A high-performance potassium metal battery using safe ionic liquid electrolyte. Proceedings of the National Academy of Sciences of the United States of America, 2020, 117, 27847-27853.	3.3	49
18	Resolving the Phase Instability of a Fluorinated Ether, Carbonate-Based Electrolyte for the Safe Operation of an Anode-Free Lithium Metal Battery. ACS Applied Energy Materials, 2020, 3, 10722-10733.	2.5	26

#	Article	IF	CITATIONS
19	Quantification of antibody avidities and accurate detection of SARS-CoV-2 antibodies in serum and saliva on plasmonic substrates. Nature Biomedical Engineering, 2020, 4, 1188-1196.	11.6	77
20	Diagnosis and prognosis of myocardial infarction on a plasmonic chip. Nature Communications, 2020, 11, 1654.	5.8	83
21	Hierarchical 3D Architectured Ag Nanowires Shelled with NiMn-Layered Double Hydroxide as an Efficient Bifunctional Oxygen Electrocatalyst. ACS Nano, 2020, 14, 1770-1782.	7.3	145
22	High-Rate and Long-Cycle Stability with a Dendrite-Free Zinc Anode in an Aqueous Zn-Ion Battery Using Concentrated Electrolytes. ACS Applied Energy Materials, 2020, 3, 4499-4508.	2.5	95
23	Electroreduction of CO ₂ to Formate on a Copper-Based Electrocatalyst at High Pressures with High Energy Conversion Efficiency. Journal of the American Chemical Society, 2020, 142, 7276-7282.	6.6	165
24	A mini-review on rare-earth down-conversion nanoparticles for NIR-II imaging of biological systems. Nano Research, 2020, 13, 1281-1294.	5.8	105
25	Highâ€Safety and Highâ€Energyâ€Density Lithium Metal Batteries in a Novel Ionicâ€Liquid Electrolyte. Advanced Materials, 2020, 32, e2001741.	11.1	176
26	Recent Advances in Development of NIR-II Fluorescent Agents. , 2020, , 83-101.		4
27	Effects of Concentrated Salt and Resting Protocol on Solid Electrolyte Interface Formation for Improved Cycle Stability of Anode-Free Lithium Metal Batteries. ACS Applied Materials & Interfaces, 2019, 11, 31962-31971.	4.0	58
28	A safe and non-flammable sodium metal battery based on an ionic liquid electrolyte. Nature Communications, 2019, 10, 3302.	5.8	173
29	Plasmonic gold chips for the diagnosis of Toxoplasma gondii, CMV, and rubella infections using saliva with serum detection precision. European Journal of Clinical Microbiology and Infectious Diseases, 2019, 38, 883-890.	1.3	22
30	Dual electrolyte additives of potassium hexafluorophosphate and tris (trimethylsilyl) phosphite for anode-free lithium metal batteries. Electrochimica Acta, 2019, 316, 52-59.	2.6	70
31	Light-sheet microscopy in the near-infrared II window. Nature Methods, 2019, 16, 545-552.	9.0	151
32	Molecular Imaging in the Second Nearâ€Infrared Window. Advanced Functional Materials, 2019, 29, 1900566.	7.8	125
33	Concentrated Dual-Salt Electrolyte to Stabilize Li Metal and Increase Cycle Life of Anode Free Li-Metal Batteries. Journal of the Electrochemical Society, 2019, 166, A1501-A1509.	1.3	104
34	Rechargeable aluminum batteries: effects of cations in ionic liquid electrolytes. RSC Advances, 2019, 9, 11322-11330.	1.7	66
35	Nearâ€Infraredâ€II Molecular Dyes for Cancer Imaging and Surgery. Advanced Materials, 2019, 31, e1900321.	11.1	631
36	Solar-driven, highly sustained splitting of seawater into hydrogen and oxygen fuels. Proceedings of the National Academy of Sciences of the United States of America, 2019, 116, 6624-6629.	3.3	524

#	Article	IF	CITATIONS
37	Highly active oxygen evolution integrated with efficient CO ₂ to CO electroreduction. Proceedings of the National Academy of Sciences of the United States of America, 2019, 116, 23915-23922.	3.3	58
38	In vivo molecular imaging for immunotherapy using ultra-bright near-infrared-IIb rare-earth nanoparticles. Nature Biotechnology, 2019, 37, 1322-1331.	9.4	398
39	Magnetic "Squashing―of Circulating Tumor Cells on Plasmonic Substrates for Ultrasensitive NIR Fluorescence Detection. Small Methods, 2019, 3, 1800474.	4.6	52
40	Site Activity and Population Engineering of NiRu-Layered Double Hydroxide Nanosheets Decorated with Silver Nanoparticles for Oxygen Evolution and Reduction Reactions. ACS Catalysis, 2019, 9, 117-129.	5.5	103
41	Robust and conductive MagnéliÂPhase Ti4O7 decorated on 3D-nanoflower NiRu-LDH as high-performance oxygen reduction electrocatalyst. Nano Energy, 2018, 47, 309-315.	8.2	59
42	Molecular Cancer Imaging in the Second Nearâ€Infrared Window Using a Renalâ€Excreted NIRâ€I Fluorophoreâ€Peptide Probe. Advanced Materials, 2018, 30, e1800106.	11.1	115
43	Donor Engineering for NIR-II Molecular Fluorophores with Enhanced Fluorescent Performance. Journal of the American Chemical Society, 2018, 140, 1715-1724.	6.6	379
44	3D NIRâ€II Molecular Imaging Distinguishes Targeted Organs with Highâ€Performance NIRâ€II Bioconjugates. Advanced Materials, 2018, 30, e1705799.	11.1	150
45	A bright organic NIR-II nanofluorophore for three-dimensional imaging into biological tissues. Nature Communications, 2018, 9, 1171.	5.8	353
46	Developing a Bright NIRâ€II Fluorophore with Fast Renal Excretion and Its Application in Molecular Imaging of Immune Checkpoint PDâ€L1. Advanced Functional Materials, 2018, 28, 1804956.	7.8	85
47	An operando X-ray diffraction study of chloroaluminate anion-graphite intercalation in aluminum batteries. Proceedings of the National Academy of Sciences of the United States of America, 2018, 115, 5670-5675.	3.3	109
48	Nearâ€Infrared IIb Fluorescence Imaging of Vascular Regeneration with Dynamic Tissue Perfusion Measurement and High Spatial Resolution. Advanced Functional Materials, 2018, 28, 1803417.	7.8	107
49	Bright quantum dots emitting at â^1⁄41,600 nm in the NIR-IIb window for deep tissue fluorescence imaging. Proceedings of the National Academy of Sciences of the United States of America, 2018, 115, 6590-6595.	3.3	310
50	Molecular imaging of biological systems with a clickable dye in the broad 800- to 1,700-nm near-infrared window. Proceedings of the National Academy of Sciences of the United States of America, 2017, 114, 962-967.	3.3	230
51	High Coulombic efficiency aluminum-ion battery using an AlCl ₃ -urea ionic liquid analog electrolyte. Proceedings of the National Academy of Sciences of the United States of America, 2017, 114, 834-839.	3.3	306
52	Rational Design of Molecular Fluorophores for Biological Imaging in the NIRâ€II Window. Advanced Materials, 2017, 29, 1605497.	11.1	356
53	Near-infrared fluorophores for biomedical imaging. Nature Biomedical Engineering, 2017, 1, .	11.6	1,982
54	Diagnosis of Zika virus infection on a nanotechnology platform. Nature Medicine, 2017, 23, 548-550.	15.2	130

#	Article	IF	CITATIONS
55	A high quantum yield molecule-protein complex fluorophore for near-infrared II imaging. Nature Communications, 2017, 8, 15269.	5.8	458
56	Autoantibody profiling on a plasmonic nano-gold chip for the early detection of hypertensive heart disease. Proceedings of the National Academy of Sciences of the United States of America, 2017, 114, 7089-7094.	3.3	30
57	Boosting the down-shifting luminescence of rare-earth nanocrystals for biological imaging beyond 1500 nm. Nature Communications, 2017, 8, 737.	5.8	416
58	Proteoliposome-based full-length ZnT8 self-antigen for type 1 diabetes diagnosis on a plasmonic platform. Proceedings of the National Academy of Sciences of the United States of America, 2017, 114, 10196-10201.	3.3	31
59	A novel quantitative microarray antibody capture assay identifies an extremely high hepatitis delta virus prevalence among hepatitis B virus–infected mongolians. Hepatology, 2017, 66, 1739-1749.	3.6	74
60	Traumatic Brain Injury Imaging in the Second Nearâ€Infrared Window with a Molecular Fluorophore. Advanced Materials, 2016, 28, 6872-6879.	11.1	311
61	Multiplexed Anti-Toxoplasma IgG, IgM, and IgA Assay on Plasmonic Gold Chips: towards Making Mass Screening Possible with Dye Test Precision. Journal of Clinical Microbiology, 2016, 54, 1726-1733.	1.8	29
62	High Performance, Multiplexed Lung Cancer Biomarker Detection on a Plasmonic Gold Chip. Advanced Functional Materials, 2016, 26, 7994-8002.	7.8	84
63	A small-molecule dye for NIR-II imaging. Nature Materials, 2016, 15, 235-242.	13.3	1,314
64	Carbon Nanomaterials for Biological Imaging and Nanomedicinal Therapy. Chemical Reviews, 2015, 115, 10816-10906.	23.0	1,151
65	An ultrafast rechargeable aluminium-ion battery. Nature, 2015, 520, 324-328.	13.7	1,970
66	Biological imaging without autofluorescence in the second near-infrared region. Nano Research, 2015, 8, 3027-3034.	5.8	263
67	Fluorescence Imaging In Vivo at Wavelengths beyond 1500â€nm. Angewandte Chemie - International Edition, 2015, 54, 14758-14762.	7.2	310
68	A mini review of NiFe-based materials as highly active oxygen evolution reaction electrocatalysts. Nano Research, 2015, 8, 23-39.	5.8	1,201
69	Graphene Nanoribbons Under Mechanical Strain. Advanced Materials, 2015, 27, 303-309.	11.1	36
70	Through-skull fluorescence imaging of the brain in a new near-infrared window. Nature Photonics, 2014, 8, 723-730.	15.6	829
71	A plasmonic chip for biomarker discovery and diagnosis of type 1 diabetes. Nature Medicine, 2014, 20, 948-953.	15.2	142
72	Recent advances in zinc–air batteries. Chemical Society Reviews, 2014, 43, 5257-5275.	18.7	1,882

#	Article	IF	CITATIONS
73	Ultrafast fluorescence imaging in vivo with conjugated polymer fluorophores in the second near-infrared window. Nature Communications, 2014, 5, 4206.	5.8	470
74	An Advanced Ni–Fe Layered Double Hydroxide Electrocatalyst for Water Oxidation. Journal of the American Chemical Society, 2013, 135, 8452-8455.	6.6	2,498
75	Multifunctional in vivo vascular imaging using near-infrared II fluorescence. Nature Medicine, 2012, 18, 1841-1846.	15.2	836
76	Chirality Enriched (12,1) and (11,3) Single-Walled Carbon Nanotubes for Biological Imaging. Journal of the American Chemical Society, 2012, 134, 16971-16974.	6.6	162
77	Three-dimensional imaging of single nanotube molecule endocytosis on plasmonic substrates. Nature Communications, 2012, 3, 700.	5.8	76
78	Ag ₂ S Quantum Dot: A Bright and Biocompatible Fluorescent Nanoprobe in the Second Near-Infrared Window. ACS Nano, 2012, 6, 3695-3702.	7.3	669
79	Graphene nanoribbons with smooth edges behave as quantum wires. Nature Nanotechnology, 2011, 6, 563-567.	15.6	197
80	Graphene Nanoribbons from Unzipped Carbon Nanotubes: Atomic Structures, Raman Spectroscopy, and Electrical Properties. Journal of the American Chemical Society, 2011, 133, 10394-10397.	6.6	170
81	Plasmonic substrates for multiplexed protein microarrays with femtomolar sensitivity and broad dynamic range. Nature Communications, 2011, 2, 466.	5.8	221
82	Deep-tissue anatomical imaging of mice using carbon nanotube fluorophores in the second near-infrared window. Proceedings of the National Academy of Sciences of the United States of America, 2011, 108, 8943-8948.	3.3	817
83	Etching and narrowing of graphene from the edges. Nature Chemistry, 2010, 2, 661-665.	6.6	441
84	Facile synthesis of high-quality graphene nanoribbons. Nature Nanotechnology, 2010, 5, 321-325.	15.6	757
85	Narrow graphene nanoribbons from carbon nanotubes. Nature, 2009, 458, 877-880.	13.7	2,313
86	A route to brightly fluorescent carbon nanotubes for near-infrared imaging in mice. Nature Nanotechnology, 2009, 4, 773-780.	15.6	1,068
87	Nano-graphene oxide for cellular imaging and drug delivery. Nano Research, 2008, 1, 203-212.	5.8	3,043
88	Room-Temperature All-Semiconducting Sub-10-nm Graphene Nanoribbon Field-Effect Transistors. Physical Review Letters, 2008, 100, 206803.	2.9	1,345
89	Chemically Derived, Ultrasmooth Graphene Nanoribbon Semiconductors. Science, 2008, 319, 1229-1232.	6.0	4,504
90	Circulation and long-term fate of functionalized, biocompatible single-walled carbon nanotubes in mice probed by Raman spectroscopy. Proceedings of the National Academy of Sciences of the United States of America, 2008, 105, 1410-1415.	3.3	1,037

#	Article	IF	CITATIONS
91	In vivo biodistribution and highly efficient tumour targeting of carbon nanotubes in mice. Nature Nanotechnology, 2007, 2, 47-52.	15.6	1,384